NON-INVASIVE BLOOD PRESSURE MONITORING
WITH MULTI-MODAL IN-EAR SENSING

Hoang Truong, Alessandro Montanari, Fahim Kawsar

Nokia Bell Labs, Cambridge (UK)

ABSTRACT

Continuous blood pressure monitoring is the key to mitigate significant risks for stroke, heart failure and coronary artery disease. Current gold-standard blood pressure devices cause discomfort and interfere with users' activities. This paper explores an earable system, which continuously monitors users' blood pressure from the ear. We propose a measurement technique based on the vascular transit time which utilises the time difference between the S1 heart sound and the PPG upstroke in one pulse cycle. We develop a multi-modal sensing hardware and processing pipeline and we evaluate it with 10 participants showing average errors in line with the range recommended by the Association for the Advancement of Medical Instrumentation: 4.07 mmHg for systolic and 5.61 mmHg for diastolic blood pressure.

Index Terms— Blood pressure, heart sounds, in-ear microphone (in-ear PCG), photoplethysmography (PPG), cuffless.

1. INTRODUCTION

Hypertension (high blood pressure) causes hundreds of thousands of deaths every year and is a significant risk factor for health conditions such as stroke, heart failure and coronary artery diseases [1, 2]. Frequent blood pressure (BP) measurements can help with early diagnosis and reduce the risks associated with high or low blood pressure.

Catheterization is the gold standard for measuring BP, however, it is invasive and requires expertise since it involves inserting a sensor inside an artery [3]. Non-invasive methods such as auscultation and oscillometry [4], instead, employ an inflatable cuff around the arm to occlude the artery while measuring. Artery occlusion can also be achieved by partially blocking the artery through an inflatable balloon inside the ear [5]. However, cuffs and ear-worn pumps are uncomfortable to wear, slow and occasionally painful. Additionally, even if ambulatory BP devices exist, they disrupt daily activities. All these factors contribute to the limited applicability of cuff-based BP monitoring for longitudinal and frequent measurements.

Common cuffless methods are based on pulse arrival/transit time (PAT or PTT), which refer to the time taken by a pulse wave to travel between two body locations [6]. However, PAT-based methods are not accurate due to the pre-ejection period variability, i.e., the delay between the appearance of the electrical signal on the electrocardiogram (ECG) and the opening of the aortic valve [6]. Additionally, PAT/PTT techniques require multiple sensing devices on the body, typically an ECG on the chest and a photoplethysmography sensor (PPG) on a peripheral location. Some works experimented with positioning sensors in or around the ear but still had to rely on other devices on the body to estimate BP such as SCG [7], BCG [8], multi-site PPG [9], or bio-impedance [10]. Other works employed cumbersome ECG electrodes attached to the neck below the ear or behind the head [11, 12]. These approaches however, increase system complexity and limit usability.

We overcome the aforementioned issues by exploiting the different propagation times of sound and blood through the human body and estimate blood pressure from a single device in the ear. The ear is a remarkable location to measure not only blood pressure but also a plethora of other vital signs (e.g., heart rate and blood oxygen saturation). The recent popularity of ear-worn devices (i.e, earables) and earbuds with in-ear microphones or PPG sensor integration makes them a perfect avenue for unobtrusive BP monitoring [13, 14].

The key to our approach is embedding an in-ear microphone and a PPG sensor in the same earable device. This multi-modal approach can measure the vascular transit time (VTT). VTT is the delay between the moment the heart starts pumping blood (denoted by the first heart sound, S1) and the upstroke of the corresponding PPG signal (Figure 1). Since the sound generated from the heart pumping blood travels through the body faster than the blood moving through the vessels, we can record the acoustic signal and PPG waveform from the same location on the body. We then identify the best markers for the two main heart sounds in the in-ear acoustic signal and propose a pipeline for their detection. Once we determine the vascular transit time, we devise two models to continuously estimate the systolic (SBP) and diastolic (DBP) blood pressure. Our approach represents a stepping stone towards the non-invasive measurement of BP from a single device exploiting an additional advantage, over the PAT-based methods, since the VTT technique is not affected by the PEP variability [15].

In summary, the contributions of this paper are:

- We develop a wearable device to simultaneously capture in-ear acoustic and PPG signals.

- We propose a signal processing pipeline and analytical models to estimate SBP and DBP from the VTT and the timing of the heart sounds measured from our in-ear device.

- We evaluate the performance of our approach with 10 participants demonstrating a mean absolute error of 4.07 mmHg and 5.61 mmHg for SBP and DBP, respectively. This result is in line with AAMI precision range recommendation. [16].

2. IN-EAR BLOOD PRESSURE MONITORING

The ear represents a perfect location for measuring blood pressure. First, earables are becoming part of everyday life. Recently, they are also living through a growing interest in healthcare and clinical research [5, 13]. Second, ears have a dense vascular structure that in combination with high blood perfusion enables the extraction of a wealth of information from blood movements (e.g., heart rate, blood oxygen saturation and respiration rate) [14]. Third, the ear canal offers a unique location to detect internal body sounds that would be otherwise difficult to record. Finally, the head is generally less sus-
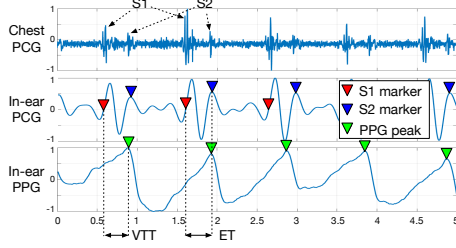
Fig. 1: Signals recorded from the chest and the ear showing vascular transmit time (VTT) and ejection time (ET) intervals.

ceptible to motion artefacts due to the musculoskeletal system's natural vibration damping and is at a fixed distance from the heart, both essential features for high accuracy BP measurements. These considerations motivated our work in estimating BP with a non-invasive earable device.

2.1. Method Overview

In this work, for the first time, we aim to estimate BP from VTT and ejection time (ET) [17] taken from a single in-ear device. Referring to Figure 1, the VTT is the time delay between the first heart sound (S1) and the upstroke of the corresponding pulse wave (measured from a PPG sensor), while the ET is the time difference between the first (S1) and the second heart sound (S2). The heart sounds are produced by the closing of the heart valves during the systolic (S1) and diastolic (S2) cycles and propagate through the body. Previous works have estimated VTT using a phonocardiography sensor (PCG) on the chest, to record heart sounds, and a PPG sensor at the fingertip, to record the blood movement and the pulse waveform [18]. Recording the PCG signal at the chest ensures good quality signals for heart sounds, however, the classic setup is limited in terms of mobility because of the multiple sensing devices that a person needs to use (one on the chest and one on the finger). Thus, a less obtrusive and mobile sensor setup for the VTT-based method is needed.

In our approach, we rely on the different propagation times of sound and blood in the human body. The sound generated from the heart travels through the body at an average speed of 1500 m/s [19], much higher than the blood movement in the arteries (in the order of tens of cm/s) [20]. Hence, we propose to record the acoustic signal (in-ear PCG) and PPG waveform from the ear and measure the VTT which we then employ to estimate the BP. However, achieving this with an earable device comes with the following challenges:

- Integrating a microphone and a PPG sensor in an earable while ensuring good signal quality (i.e., stable PPG sensor contact and proper ear canal seal) is not trivial.

- Identifying S1 and S2 heart sounds from in-ear acoustic signals is challenging as the body heavily attenuates and distorts the signal as it travels through tissues and organs [21]. Figure 1 shows how S1 and S2 are clearly visible from the chest recording. The in-ear recording presents a significantly different signal where the accurate detection of the two sounds and their relative timing is not obvious.

- While VTT has a linear relationship with SBP, DBP does not have such clear formulation and requires other parameters to estimate.

2.2. Prototype Wearable Device

For our prototype (Figure 2), we select the InvenSense ICS-40330 analog microphone [22] due to its extended low frequency response. The microphone is positioned inside an existing earbud casing facing
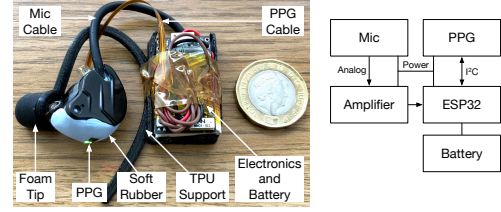

Fig. 2: Prototype device with in-ear PCG and PPG sensors.

towards the ear canal. The signal is amplified with an amplifier built around the MAX4466 [23] and then sampled at 16kHz by an ESP32 microcontroller [24]. The PPG signal is acquired at a frequency of 100Hz by a MAXM86161 [25] which is connected to the ESP32 via I^2C. The PPG sensor can record data at three wavelengths, green (530nm), red (660nm) and infrared (880nm), however, for our experiments we use only the infrared wavelength.

Our prototype weighs 18g and allows the replacement of the ear tips inserted into the ear canal. We use foam tips of different sizes to suit the characteristics of each participant. This ensures a comfortable experience while guaranteeing a good seal of the ear canal which improves the SNR of the acoustic signal. The positioning of the PPG has been also carefully chosen to enable consistent measurements across participants. The sensor sits inside the concha, in the outer ear, and points towards the antitragus which ensures a good contact with the skin and shields the sensor from ambient light.

2.3. Heart Sounds Detection and VTT Estimation

We continuously process the raw data using a sliding window of 10 seconds with 90% overlap following the processing pipeline in Figure 3. We remove the DC linear drifting in both in-ear PCG and PPG signals by excluding the 6th-order polynomial fit from each sub-window of 2.5 seconds in the current processing window. Then each signal follows the pipeline differently to find the exact location of S1, S2 sounds and the systolic peak in their time domain.
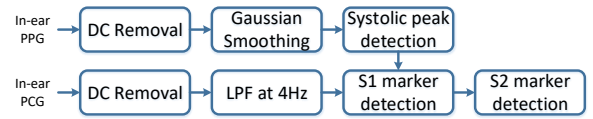

Fig. 3: In-ear PCG and PCG processing pipeline.

In-ear PPG systolic peak detection. Each cardiac cycle ejects blood into the aorta which then propagates throughout the body. The arrival of the blood at the arterial branches under the PPG sensor creates a local peak on the PPG signal, called the systolic peak. Firstly, we apply a Gaussian smoothing to remove high-frequency noise in the detrended in-ear PPG signal, yet preserve the signal magnitude. Then we use a peak detection algorithm within each predefined non-overlapping sub-window to find the maximum of that sub-window and mark it as the corresponding systolic peak.

In-ear PCG Forward-Backward Filtering. Since the normal heartbeat range is 40-180 bpm, S1 and S2 happen at a frequency below 3 Hz. Hence, we will need to apply a low-pass filter to extract this frequency range of interest. However, using a low-pass filter normally creates a time delay in the output signal and leads to inaccuracies in detecting the exact location of S1 and S2 heart sounds. This would lead to the wrong measurement of the VTT and ET, resulting in poor performance for BP estimation. Thus, we look for a proper filtering technique to ensure no phase distortion and time delay and focus on the forward-backward filtering.
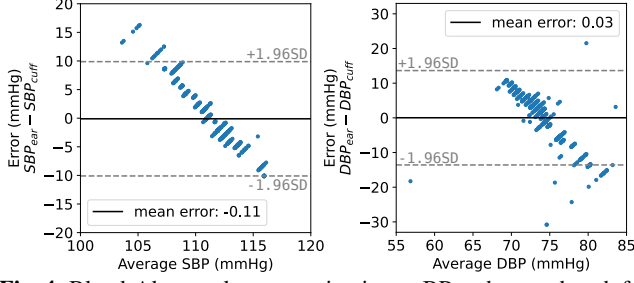
Fig. 4: Bland-Altman plot comparing in-ear BP and ground truth for the leave-one-user-out cross-validation.

Fig. 5: Bland-Altman plot comparing in-ear BP and ground truth for the personalised models evaluation.

Let $p_{raw}[n]$ and $P_{raw}(e^{j\omega})$ be our in-ear PCG signal in time and frequency domain. After applying a filter $h[n]$ with transfer function $H(e^{j\omega})$ (i.e. forward direction), we receive: $p_{fw}[n] = h[n] * p_{raw}[n]$ with $P_{fw}(e^{j\omega}) = H(e^{j\omega})P_{raw}(e^{j\omega})$.

Then we take its time-reversal and apply the same filter (i.e., backward direction) to get $p_{bw}[n] = h[n] * p_{fw}[-n]$ with $P_{bw}(e^{j\omega}) = H(e^{j\omega})P_{fw}^{*}(e^{j\omega})$.

We take the time-reversal of $p_{bw}[n]$ to get the final output:

$$P_{fil}(e^{j\omega}) = P_{bw}^{*}(e^{j\omega}) = |H(e^{j\omega})|^2 P_{raw}(e^{j\omega}) \tag{1}$$

We then apply this technique on each sliding window with a 4 Hz low-pass filter on our in-ear PCG signal. The overall effective transfer function, $|H(e^{j\omega})|^2$, introduces zero phase and no time delay. These characteristics help preserve features in a filtered time waveform exactly where they occur in the unfiltered original signal. **S1 & S2 marker detection.** S1 and S2 heart sounds create two pairs of consecutive local negative peak and local positive peak in each cardiac cycle of the filtered in-ear PCG signal, as visible in Figure 1. These two pairs are followed by a PPG systolic peak in the same cycle. Thus, we use that systolic peak as a pivot and search for the 2 local maxima within its adjacent location. We then use those two local maxima to search for the two corresponding local minima. From our empirical observation, we locate the S1 marker at the zero-crossing point of the peak pair which happens first in the time domain, and the S2 marker at the positive peak of the remaining pair. Finally, the VTT and ET are calculated as the time differences between systolic peak & S1 marker, and S2 & S1 markers, respectively.

2.4. Blood Pressure Model

Systolic Blood Pressure. The change in systolic blood pressure measurement is correlated to the change in VTT [17]. Thus, the SBP is usually related to the VTT by the linear approximation:

$$SBP \approx \alpha_1 VTT + \alpha_0 \tag{2}$$

Diastolic Blood Pressure. The diastolic blood pressure instead, is not directly related to VTT but it can be inferred from the SBP and the Pulse Pressure (PP), which is the difference between SBP and DBP, as $DBP = SBP - PP$. This poses the problem of how to estimate PP.

Previous studies [26] proposed the relationship between PP and Stroke Volume (SV) and the aortic root compliance C as $PP = SV/C$. Stroke volume is the volume of blood ejected from each ventricle due to the contraction of the heart and is shown to have a linear relationship with Ejection Time (ET) [27]: $SV = \beta_1 ET + \beta_0$.

Since VTT is considered as the time taken for a pulse wave to travel along an arterial tube with length l: $VTT = l\sqrt{\rho C/A}$, where ρ is the fluid density, A and C are the cross-sectional area and compliance of the tube, respectively.
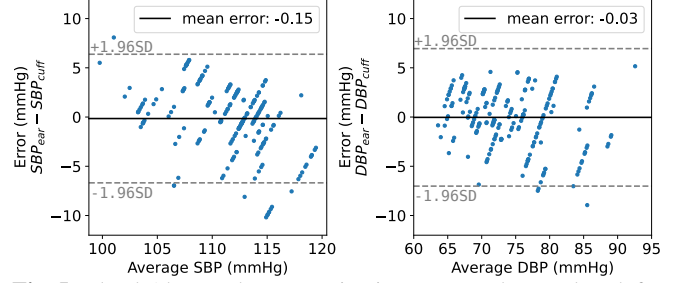
Thus we can re-write PP as:

$$PP = \frac{SV}{C} = \frac{\beta_1 ET + \beta_0}{\frac{A}{\rho l^2} VTT^2}$$

Because A, ρ, C are user-specific parameters, we propose to estimate the pulse pressure as:

$$PP \approx \gamma_1 \frac{ET}{VTT^2} + \gamma_2 \frac{1}{VTT^2} + \gamma_0 \tag{3}$$

Following the VTT and ET calculation in §2.3, we calibrate our sysem with a BP groud truth device and estimate α_- and γ_- coefficients using least-square fitting algorithm from equation 2 and 3. While other works have derived similar relationships for PP based on PTT, here we propose a formulation based on VTT and ET and we show its effectiveness for the estimation of DBP. This model represents a baseline approach that fits well with the preliminary nature of the work. A more sophisticated model with various parameters (such as age, weight, height) [28] or machine learning models can be applied. However, these approaches require a larger amount of data to work properly. We aim to evaluate them in future work, after we deploy our device to a larger population.

3. EVALUATION

3.1. Data Collection and Evaluation Procedure

Participants. We recruited 10 participants (2 females, avg. age = 29.6, std = 3.17). All participants were in good health and had no heart or blood pressure condition. They were briefed about the study and voluntarily consented to take part in it (compensation of $10). The study received IRB approval before its beginning.

Protocol. The participants were asked to wear our wearable prototype on the left ear and the cuff for BP measurement on the left arm. Since clinical-grade continuous BP measurements require invasive techniques like catheterization, we opted for an accurate but conventional monitoring device that relies on a cuff for the measurement. For this purpose, we used the Omron M7 Intelli IT [29] to measure the BP ground truth. Additionally, we attached a stethoscope connected to a microphone to record the heart sounds directly from the chest and compare them with the in-ear recordings.

For the entire duration of the experiment, the participants remained seated, with their feet and back supported. In order to induce temporary changes in the participants' BP, we asked them to perform two activities. The first one consists in taking slow and deep breaths, this has been shown to lower the BP [30], and the second one involves raising the BP temporarily by dipping the right hand in cold water [31]. We do not use the valsava maneuver method because, during a pre-study analysis, we found it to cause discomfort in the participants. Ground truth BP measurements were taken during and
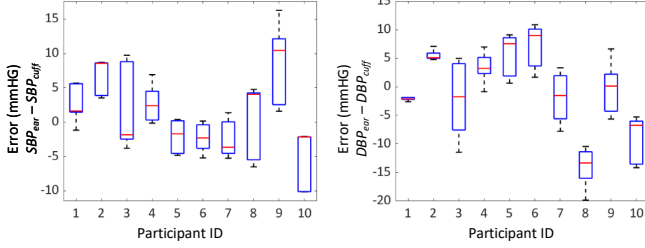
Fig. 6: BP error distributions for each participant for the leave-one-user-out cross-validation.

Fig. 7: BP error distributions for each participant for the personalised models evaluation.

Fig. 8: BP variations during the data collection from 1 participant.

after each activity, in addition to one measurement at the very beginning of the session, resulting in a total of 5 measurements per participant. Meanwhile, the in-ear device and chest microphone recorded data continuously for the entire session. There are 769 data points in total after outlier removal. The groundtruth SBP is in the range [103 130] with mean of 113 and std of 6.4. The groundtruth DBP is in the range [64 109] with mean of 77.9 and std of 12.

Evaluation procedure. The data collected from our prototype is processed following the approach proposed in §2 to estimate SBP_{ear} and DBP_{ear}. Since the ground truth (i.e., SBP_{cuff} and DBP_{cuff}) is not continuous and it takes around 30 seconds for the ground truth device to finish the BP measurement, we assume the BP values are the same for this 30-second window. To build our dataset we use the sensor data (PPG and microphone) from 15s before and 15s after the timestamp at which the GT BP measurement was taken.

Further, two evaluation methodologies are followed. Firstly, we adopt a leave-one-user-out cross-validation approach where data from 9 users is used to fit the BP estimation models (see § 2.4) while the data from the remaining user is used for evaluation. This approach gives an indication of performance on unseen data from different participants. Secondly, we build personalised models for each participant by using 70% of the data to fit the model and the remaining to evaluate its performance. This method provides insights into the potential benefits of user-specific calibration. For both approaches, we use mean error (ME), mean absolute error (MAE) and standard deviation of the errors (SD) as evaluation metrics.

3.2. Results

Aggregated Analysis. Figures 4 and 5 show the results for all participants for the leave-one-user-out (LOUO) and personalised models evaluation, respectively. For both evaluation approaches, we notice that the mean error ($BP_{ear} - BP_{cuff}$) is very close to zero, with few datapoints outside the confidence intervals (±1.96 of the standard deviation of the error). However, in the LOUO case, the datapoints are more sparse compared to the personalised models, indicating larger error variations. Table 1 summarises the errors for the two evaluation approaches. In both cases, the mean error and standard deviation are in line with the AAMI recommendations (BP estimation mean error should be less than $5.0 ± 8.0$ mmHg).

Table 1: Metrics for the two evaluation approaches (see §3.1).

	Leave One User Out		Personalised Models	
	ME (SD)	MAE (SD)	ME (SD)	MAE (SD)
SBP	-0.11 (5.10)	4.07 (3.07)	-0.15 (3.34)	2.50 (2.20)
DBP	0.03 (6.95)	5.61 (4.09)	-0.03 (3.57)	2.42 (2.62)

Individual Participant Analysis. We delve deeper by plotting the error distributions for each participant in Figures 6 and 7 for the LOUO and personal models evaluation, respectively. From Figure 6 we observe large error variations across different participants, in particular for the DBP estimation. For some participants the median
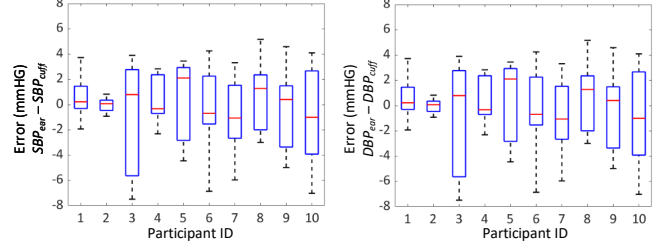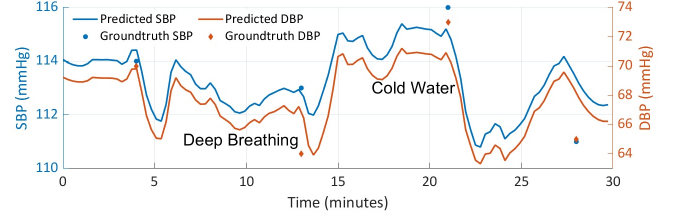
error is low with limited interquartile range, while others have large median errors and the values are spread further apart. We hypothesise this might be caused by the limited sample size and hence the limited generalisation to all participants. This is particularly true for participants 8, 9 and 10, who have the largest error variations.

Figure 7 instead shows how using data from the same participant to calibrate the BP estimation models results in lower median errors and less error variation. The better performance of the personalised models compared to the LOUO evaluation is expected since the latter is more challenging given that the fitted model is tested on unseen data from a different participant. This suggests that calibrating the BP model for each participant would likely yield better accuracy since the model would account for individual characteristics. However, the frequency at which the calibration needs to be performed remains an open research problem which goes beyond the scope of this work. We aim to consider it in future work.

Qualitative Visualisation. Figure 8 provides a visualisation of how the combination of our earable device and processing technique provides a continuous BP estimate over time. From the figure we can observe how the two activities performed by the participant resulted in BP changes. The deep breathing exercise results in a slow and gradual lowering of the BP which takes a few minutes, while dipping the hand in clod water creates a quicker response in the participant's BP. Our empirical evaluation suggests that we can accurately measure BP through the proposed S1 and S2 markers and analytical models, therefore our system represents a promising solution for in-ear non-invasive BP monitoring.

4. CONCLUSIONS

We presented a non-invasive BP estimation technique based on vascular transit time measured, for the first time, exclusively from the ear. Our intial results with 10 participants are promising, with mean absolute errors of 4.07 mmHg and 5.61 mmHg for SBP and DBP, respectively, both aligned with the AAMI precision range recommendation. We acknowledge that the limited sample size and the controlled experimental settings are limitations of this work. We aim to address both in future work by collecting additional data and exploring the effect of external noise and movement. Nevertheless, we believe this work is a step towards unobtrusive BP monitoring with earables.

5. REFERENCES

[1] "World Health Organization - Hypertension," https://tinyurl.com/hyperfact, 2021.

[2] "Centers for Disease Control and Prevention - Facts About Hypertension," https://www.cdc.gov/bloodpressure/facts.html, 2021.

[3] B. H. McGhee and E. J. Bridges, "Monitoring arterial blood pressure: what you may not know," *Critical care nurse*, vol. 22, no. 2, pp. 60–79, 2002.

[4] A. S. Meidert and B. Saugel, "Techniques for non-invasive monitoring of arterial blood pressure," *Frontiers in medicine*, vol. 4, pp. 231, 2018.

[5] N. Bui, N. Pham, J. J. Barnitz, Z. Zou, P. Nguyen, H. Truong, T. Kim, N. Farrow, A. Nguyen, J. Xiao, et al., "eBP: A wearable system for frequent and comfortable blood pressure monitoring from user's ear," in *The 25th annual international conference on mobile computing and networking*, 2019, pp. 1–17.

[6] M. Elgendi, R. Fletcher, Y. Liang, N. Howard, N. H. Lovell, D. Abbott, K. Lim, and R. Ward, "The use of photoplethysmography for assessing hypertension," *NPJ digital medicine*, vol. 2, no. 1, pp. 1–11, 2019.

[7] C. Yang and N. Tavassolian, "Pulse transit time measurement using seismocardiogram, photoplethysmogram, and acoustic recordings: Evaluation and comparison," *IEEE journal of biomedical and health informatics*, vol. 22, no. 3, pp. 733–740, 2017.

[8] C.-S. Kim, A. M. Carek, R. Mukkamala, O. T. Inan, and J.-O. Hahn, "Ballistocardiogram as proximal timing reference for pulse transit time measurement: Potential for cuffless blood pressure monitoring," *IEEE Transactions on Biomedical Engineering*, vol. 62, no. 11, pp. 2657–2664, 2015.

[9] G. Chan, R. Cooper, M. Hosanee, K. Welykholowa, P. A. Kyriacou, D. Zheng, J. Allen, D. Abbott, N. H. Lovell, R. Fletcher, et al., "Multi-site photoplethysmography technology for blood pressure assessment: challenges and recommendations," *Journal of clinical medicine*, vol. 8, no. 11, pp. 1827, 2019.

[10] B. Ibrahim and R. Jafari, "Cuffless blood pressure monitoring from an array of wrist bio-impedance sensors using subject-specific regression models: Proof of concept," *IEEE transactions on biomedical circuits and systems*, vol. 13, no. 6, pp. 1723–1735, 2019.

[11] E. S. Winokur, D. Da He, and C. G. Sodini, "A wearable vital signs monitor at the ear for continuous heart rate and pulse transit time measurements," in *2012 Annual International Conference of the IEEE Engineering in Medicine and Biology Society*. IEEE, 2012, pp. 2724–2727.

[12] Q. Zhang, X. Zeng, W. Hu, and D. Zhou, "A machine learning-empowered system for long-term motion-tolerant wearable monitoring of blood pressure and heart rate with ear-ecg/ppg," *IEEE Access*, vol. 5, pp. 10547–10561, 2017.

[13] F. Kawsar, C. Min, A. Mathur, and A. Montanari, "Earables for personal-scale behavior analytics," *IEEE Pervasive Computing*, vol. 17, no. 3, pp. 83–89, 2018.

[14] A. Ferlini, A. Montanari, C. Min, H. Li, U. Sassi, and F. Kawsar, "In-ear ppg for vital signs," *IEEE Pervasive Computing*, , no. 01, pp. 1–10, dec 5555.

[15] M. Hasegawa, D. Rodbard, and Y. Kinoshita, "Timing of the carotid arterial sounds in normal adult men: measurement of left ventricular ejection, pre-ejection period and pulse transmission time," *Cardiology*, vol. 78, no. 2, pp. 138–149, 1991.

[16] "ANSI/AAMI SP10-1992 Standard," http://www.aami.org/.

[17] J. Y. A. Foo, C. S. Lim, and P. Wang, "Evaluation of blood pressure changes using vascular transit time," *Physiological measurement*, vol. 27, no. 8, pp. 685, 2006.

[18] C.-C. Hsiao, J. Horng, R.-G. Lee, and R. Lin, "Design and implementation of auscultation blood pressure measurement using vascular transit time and physiological parameters," in *2017 IEEE International Conference on Systems, Man, and Cybernetics (SMC)*. IEEE, 2017, pp. 2996–3001.

[19] "IT'IS Foundation," https://tinyurl.com/itisswiss.

[20] M. Klarhöfer, B. Csapo, C. Balassy, J. Szeles, and E. Moser, "High-resolution blood flow velocity measurements in the human finger," *Magnetic Resonance in Medicine: An Official Journal of the International Society for Magnetic Resonance in Medicine*, vol. 45, no. 4, pp. 716–719, 2001.

[21] W. Shi and J.-C. Chiao, "Neural network based real-time heart sound monitor using a wireless wearable wrist sensor," *Analog Integrated Circuits and Signal Processing*, vol. 94, no. 3, pp. 383–393, 2018.

[22] "InvenSense ICS-40300," https://tinyurl.com/ics-40300.

[23] "Maxim Integrated MAX4466," https://tinyurl.com/MAX4466aa.

[24] "TinyPico Developer Platform," https://www.tinypico.com/.

[25] "Maxim Integrated MAXM86161," https://tinyurl.com/MAXM86161.

[26] D. Chemla, J.-L. Hébert, C. Coirault, K. Zamani, I. Suard, P. Colin, and Y. Lecarpentier, "Total arterial compliance estimated by stroke volume-to-aortic pulse pressure ratio in humans," *American journal of physiology-Heart and circulatory physiology*, vol. 274, no. 2, pp. H500–H505, 1998.

[27] A. M. Weissler, R. G. Peeler, and W. H. Roehll Jr, "Relationships between left ventricular ejection time, stroke volume, and heart rate in normal individuals and patients with cardiovascular disease," *American heart journal*, vol. 62, no. 3, pp. 367–378, 1961.

[28] S. N. Shukla, K. Kakwani, A. Patra, B. K. Lahkar, V. K. Gupta, A. Jayakrishna, P. Vashisht, and I. Sreekanth, "Noninvasive cuffless blood pressure measurement by vascular transit time," in *2015 28th International Conference on VLSI Design*. IEEE, 2015, pp. 535–540.

[29] "Omron M7 Intelli IT," https://tinyurl.com/M7Intelli.

[30] H. Mori, H. Yamamoto, M. Kuwashima, S. Saito, H. Ukai, K. Hirao, M. Yamauchi, and S. Umemura, "How does deep breathing affect office blood pressure and pulse rate?," *Hypertension research*, vol. 28, no. 6, pp. 499–504, 2005.

[31] S. Mishra, M. Manjareeka, and J. Mishra, "Blood pressure response to cold water immersion test," *International Journal of Biology, Pharmacy and Allied Sciences*, vol. 10, pp. 1483–1491, 2012.